Evidence for quaternary seismic activity of the La Alberca-Teremendo fault, Morelia region, Trans-Mexican Volcanic Belt

Diana Cinthia Soria-Caballero[1,*], Víctor Hugo Garduño-Monroy[2], María Alcalá[3], María Magdalena Velázquez-Bucio[4], and Laura Grassi[5]

[1] *Posgrado en Ciencias de la Tierra, Escuela Nacional de Estudios Superiores, unidad Morelia, Universidad Nacional Autónoma de México, Antigua Carretera a Pátzcuaro no. 8701, Ex-Hacienda de San José de La Huerta, C.P. 58190, Morelia, Michoacán, Mexico.*
[2] *Instituto de Investigaciones en Ciencias de la Tierra, Universidad Michoacana de San Nicolás de Hidalgo, Avenida Francisco J. Mújica s/n, C.P. 58030, Morelia, Michoacán, Mexico.*
[3] *Facultad de Biología, Universidad Michoacana de San Nicolás de Hidalgo, Avenida Francisco J. Mujica s/n, C.P. 58030, Morelia, Michoacán, Mexico.*
[4] *Posgrado en Geografía Ambiental, Centro de Investigación en Geografía Ambiental, Morelia, Universidad Nacional Autónoma de México, Antigua Carretera a Pátzcuaro no. 8701, Ex-Hacienda de San José de La Huerta, C.P. 58190, Morelia, Michoacán, Mexico.*
[5] *Università degli Studi di Milano-Bicocca, Piazza dei Daini, 2, 20126 Milano MI, Italy.*
** dcinthiasoriac@gmail.com*

ABSTRACT

The La Alberca-Teremendo fault is a 26 km-long, complex fault composed of an *en échelon* array of short crustal fault segments, belonging to the Morelia-Acambay fault system. This fault system shows parallel scarps with morphological evidence of recent activity such as drainage alteration, maximum throws of 50 m and minimum throws of 1.4 m that displace the recent soils. The fault acted as a conduit for the formation of the La Alberca de Guadalupe maar (23000 to 21000 years ago) and displaced afterwards its phreatomagmatic sequences. The paleoseismic analysis indicates that the La Alberca-Teremendo fault moved three times in the past 23000 years (age of the maar); this activity caused an average vertical displacement of 87 cm, and might have generated earthquakes with magnitudes M_w between 6.6 and 7, as well as volcano-tectonic earthquakes with magnitudes M_w between 4 and 5.5. The displacements were identified on the fault through the superposition of soils differentiated by a disconformity and an anomalous increase in the percentage of clay and organic matter. The La Alberca-Teremendo fault has dominant dip slip with a minor left-lateral component, a slip rate of 0.114 mm/year, and an average recurrence interval of 7726 ± 68 years. According to scaling relations that use the surface rupture length, if we assume that the La Alberca-Teremendo fault moves tectonically, it could generate earthquakes with maximum magnitudes of M_w between 6.7 and 7.3, however because of the active volcanic processes in the area, we could expect moderate volcano-tectonic earthquakes (M_w 4–5.5) rather than catastrophic ones.

Key words: Neotectonics; paleoseismology; crustal fault activity; interrupted soil; Morelia-Acambay fault system; La Alberca-Teremendo fault; Mexico.

RESUMEN

La falla La Alberca-Teremendo es una falla cortical compleja de 26 km de largo, con geometría en échelon que pertenece al Sistema de Fallas Morelia-Acambay. Esta falla muestra evidencias morfológicas de actividad vulcano-tectónica reciente, tales como: alteraciones en la red de drenaje, un escarpe bien definido que desplaza a los suelos recientes del área y además la falla actuó como un conducto facilitador para la formación del maar conocido como La Alberca de Guadalupe hace 23000 a 21000 años, desplazando las secuencias freatomagmáticas del mismo. El análisis paleosísmico indica que la falla La Alberca-Teremendo se ha movido tres veces en los últimos 23000 años (la edad del maar), ocasionando un desplazamiento vertical promedio de 87 cm y pudo haber generado sismos tectónicos con magnitudes M_w entre 6.6 y 7, así como sismos vulcano-tectónicos de magnitudes M_w entre 4 y 5.5. Estos desplazamientos en la falla fueron identificados a través de la superposición de suelos expuestos en el área de falla, diferenciados por una discordancia erosional y un incremento anómalo en los porcentajes de arcilla y materia orgánica. La falla La Alberca-Teremendo es una falla normal con una pequeña componente de desplazamiento lateral izquierdo. La falla posee una tasa de desplazamiento de 0.114 mm/año y un intervalo de recurrencia promedio de 7726 ± 68 años. De acuerdo con las relaciones empíricas resueltas en este trabajo, si la falla se moviera tectónicamente y rompiera en toda su longitud, sería capaz de generar sismos con magnitudes máximas M_w entre 6.7 y 7.3; sin embargo, debido a los procesos volcánicos activos en el área, es más probable la ocurrencia de sismos vulcano-tectónicos de magnitud moderada (M_w 4–5.5) que de sismos catastróficos.

Palabras clave: Neotectónica; paleosismología; actividad de fallas corticales; suelo interrumpido; sistema de fallas Morelia-Acambay; falla La Alberca-Teremendo; México.

INTRODUCTION

The central part of Mexico is regularly affected by earthquakes related to subduction processes, volcanic activity, and crustal faults. In the past 500 years, severe crustal earthquakes with epicenters located on faults within the Trans-Mexican Volcanic Belt (TMVB), particularly

Soria-Caballero, D.C., Garduño-Monroy, V.H., Alcalá, M., Velázquez-Bucio, M.M., Grassi, L., 2019, Evidence for quaternary seismic activity of the La Alberca-Teremendo Fault, Morelia region, Trans-Mexican Volcanic Belt: Revista Mexicana de Ciencias Geológicas, v. 36, núm. 2, p. 242-258.

 DOI: http://dx.doi.org/10.22201/cgeo.20072902e.2019.2.1092

on faults of the Chapala-Tula fault zone and the Taxco-San Miguel de Allende fault system, caused considerable human losses and material damage. Some examples are the following: in 1567, in Ameca, M_w 7.2 (Suter, 2015) or M_w 7.5–7.8 (Suárez *et al.,* 1994); in 1875, in San Cristóbal de la Barranca, M_I VII (Bárcena, 1875; Iglesias *et al.,* 1877); in 1912 in Acambay, M_w 6.8–7 (Urbina and Camacho 1913; and Langridge *et al.,* 2000); in 1920, in Xalapa, M_s 6.2–6.4 (Flores *et al.,* 1922; Suter *et al.,* 1996). In spite of these studies, crustal earthquakes have not been the objective of comprehensive researches (Zúñiga *et al.,* 2003).

The TMVB is a volcanic arc located in central Mexico, between 19°N and 21°N, formed by the interaction of the Cocos, Rivera, and North-American plates since the Miocene (Mooser, 1972; Demant, 1978; Ferrari *et al.,* 2012). The central part of the TMVB is deformed by the extensional Morelia-Acambay fault system (MAFS, Figure 1). This system belongs to the Chapala-Tula fault zone and includes some of the most active crustal faults in Mexico. This fault system is also influenced by the Quaternary activity of the Michoacán-Guanajuato Volcanic Field (Johnson and Harrison, 1990; Hasenaka and Carmichael, 1985).

Despite the seismic and paleoseismic studies carried out along the MAFS, most of the faults remain unreported and their seismogenic potential is not considered in urban planning. This omission is a serious problem considering the population increase in central Mexico. So far, paleoseismic studies have been concentrated in the eastern part of the MAFS, around the epicenter of the 1912 Acambay earthquake (Lacan *et al.*, 2018; Velázquez-Bucio and Garduño-Monroy, 2018; Ortuño *et al.*, 2019), leaving the western portion of the system with scarce information about recurrence intervals and potential magnitudes (Garduño-Monroy *et al.*, 2009; Singh *et al.*, 2012; Suter, 2016). This information is required for a reliable seismic hazard assessment throughout the system.

This work focuses on the characterization of the La Alberca-Teremendo fault activity (LATF, Figure 1) from a paleoseismic and neotectonic perspective. The seismogenic potential of the LATF has never been assessed, despite geomorphological evidence of recent activity, such as a linear escarpment inside a well-defined Quaternary graben, and displacement of soils and phreatomagmatic sequences of La Alberca de Guadalupe maar (LAG), dated as ~21 ka (Siebe *et al.,* 2014; Kshirsagar *et al.,* 2015).

The main purpose of this work is to identify and characterize the rupture events of the LATF, their potential magnitude M_w, and the associated seismic hazard. These parameters were identified via a paleoseismic analysis, emphasizing soils pedogenesis, combined with a geomorphologic characterization. We propose a work scheme that can be used for the study of other faults that displace recent soils.

BACKGROUND

The MAFS developed in a left-lateral, transtensional, stress field that accommodates deformation in the center of the TMVB, according to the oblique subduction model with slip partitioning proposed by Ego and Ansan (2002). The MAFS presents geomorphological features and superficial scarps related to historical seismicity (Suter *et al.,* 2001). Aside from the 1912 Acambay earthquake, other historical crustal earthquakes in the MAFS occurred in Pátzcuaro, in 1845 with M_I VIII (Sánchez-Garcilazo, 2000), Maravatío in 1979 with M_b = 5.3 (Astíz-Delgado, 1980; Garduño-Monroy and Gutiérrez-Negrín, 1992) and Morelia in 2007 with M_w = 4.3 (Garduño-Monroy *et al.,* 2009; Singh *et al.,* 2012). There are also some poorly-recorded seismic crises between 1750 and 1890 in the Venta de Bravo fault, and the regions of Araró and Ucareo-Zinapécuaro-Acámbaro (Arreola, 1985; Dobson and Mahood, 1985; Suter *et al.,* 1992, 1996), as well as shallow crustal seismicity in march and october, 1976 in the Mezquital graben-Los Aljibes semi-graben (Quintanar *et al.,* 2004). Additionally, an intermediate-depth,

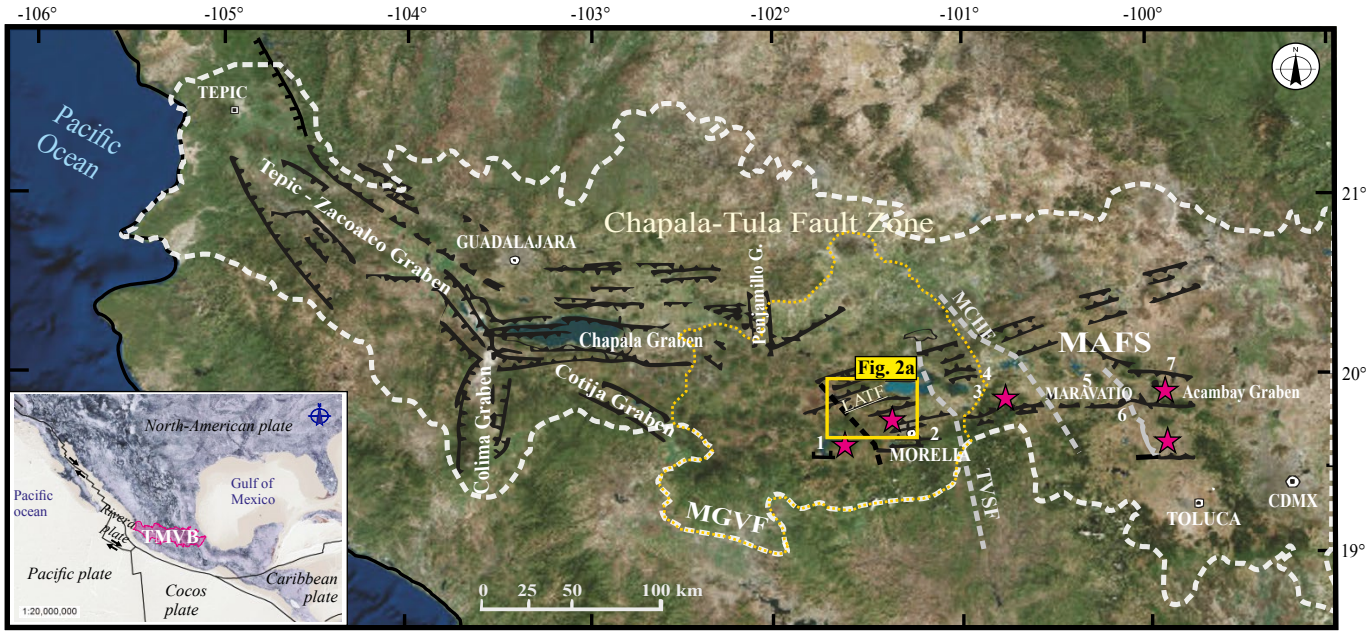

Figure 1. Location of the Trans-Mexican Volcanic Belt (TMVB), the Michoacán-Guanajuato volcanic field (MGVF; yellow, dotted line) and tectonic structures of the Chapala-Tula fault zone and the Morelia-Acambay fault system (MAFS). Stars indicate sites with published paleoseismic studies and numbers indicate historical earthquakes: 1 = Pátzcuaro, 1845 and 1858; 2 = Morelia, 2007; 3 = Araró, 1845; 4 = Ucareo-Zinapécuaro-Acámbaro, 1872 and 1874; 5 = Maravatío, 1979; 6 = Venta de Bravo, 1734–1755 and 1853–1854; 7 = Acambay, 1912. Abbreviations: TVSF, Tzitzio-Valle de Santiago inferred fault (from Garduño-Monroy *et al.*, 2009 and Arce *et al.,* 2012); MCHF, Maravatío-Ciudad Hidalgo inferred fault (from Garduño-Monroy *et al.*, 2009 and Arce *et al.,* 2012); LATF = La Alberca-Teremendo Fault; CDMX = Mexico City (Images obtained from ArcMap 10.2.2 and modified from Gómez-Tuena *et al.*, 2005).

in-slab earthquake occurred in 1858 in Pátzcuaro with M_w = 7.7 that caused severe damage in the area (Singh *et al.,* 1996) (Figure 1).

The paleoseismic studies performed in the Acambay graben show that most of the faults were active during Late Pleistocene to Holocene times, with slip rates of 0.03–0.37 mm/yr., recurrence intervals of 2000 to 15000 years, and potential seismic magnitudes (M_w) of 6.4–7.0 (Langridge *et al.,* 2000, 2013; Ortuño *et al.,* 2015; Sunye-Puchol *et al.,* 2015; Lacan *et al.,* 2018). In the Pátzcuaro-Morelia-Cuitzeo region, paleoseismic studies have been performed on fault traces and lacustrine sequences, reporting slip rates of 0.009–2.78 mm/yr., recurrence intervals of 1200 to 20000 years, and potential seismic magnitude (M_w) of 5.8–7.1 (Garduño-Monroy *et al.,* 2009; Suter, 2016).

STUDY AREA

The LATF is located in the northern part of the state of Michoacán, 30 km northwest of the capital, Morelia, within the Michoacán-Guanajuato Volcanic Field (MGVF) and the western portion of the MAFS (Figure 2). The area is a transition zone between Miocene volcanic activity and the Quaternary volcanism of the TMVB which renders the faulting poorly detectable around Cuitzeo. The oldest rocks exposed in the area are Miocene andesite (~19 Ma) and dacitic ignimbrite of the Mil Cumbres sequence, followed by a Miocene-Pliocene fluvial-lacustrine sequence of the Cuitzeo paleo-basin, Pleistocene andesite and dacite from the El Tzirate Volcanic Complex and Holocene basaltic andesite of the MGVF (Figure 2b) (Pasquarè *et al.*, 1991; Garduño-Monroy, 1999; Israde-Alcántara *et al.,* 2010; Gómez-Vasconcelos *et al.,* 2015; Pérez-Orozco *et al.,* 2018).

The La Alberca-Teremendo fault displays a complex geometry. The fault is composed of eleven segments with an *en échelon* array, separated by less than one kilometer, and individual lengths that range between 2 and 10 km; the total length of the combined segments is 26 km (Figure 2a). It could be interpreted as an immature normal fault whose segments are still not merged, but under tectonic stress could be connected; however, we need more geophysical data in order to clarify the connection between segments. The LATF trends N85°E and dips 75°NW. This structure shows predominantly dip slip, but features such as the displacement of the LAG crater and deviation of the drainage network to the left indicate a minor left-lateral displacement.

The morphological expressions of the LATF are semi-graben geometries in Cuitzeo, formed by uplifted, rotated, and tilting blocks of Miocene ignimbrite and fluvial-lacustrine sequences; a counter slope in the southern flank of El Picacho volcano; and the cut-in-half LAG maar (Figure 2c). The fault generates a maximum height throw of ~ 50 m visible on the basaltic-andesite lavas of the LAG maar basement exposed in the crater; the minimum height throw is ~ 1–1.4 m, located at the western end of the fault, where the scarp puts the maar phreatomagmatic sequences in contact with current soil.

The LATF also displays characteristics similar to magma-induced extensional structures, like a geometrical array composed by subparallel normal faults with lengths < 14 km and dips between 70°–80°, but originates fault scarps of > 2 m, and 8°–15° tilting in the hanging wall. The western limit of the fault is a NNE-SSW eruptive fissure that distributes felsic material from the El Tzirate Volcanic Complex (Pérez-Orozco *et al.,* 2018); the eastern limit is El Picacho semi-shield volcano and the faulting zone of the southern part of Cuitzeo lake, where large fault planes are observed without related dikes. The observation of dike-induced structures is more conspicuous around Queréndaro, east of the study area, where ten monogenetic cones are aligned on an E-W eruptive fracture, and internally sustained by a ~ 700 ka-old dike; here the electrical tomography displays intrusive bodies related to NNW-SSE structures (Gómez-Vasconcelos *et al.*, 2018).

The study of the LATF area must take into consideration of the influence of both, the magma-induced structures of the MGVF and the tectonic structures of the MAFS, and its extensional regime. In the area, the stress could be accommodated either by magmatism, normal faulting, or both, and the evaluation of the activity could be problematic. We consider that, in the study area, magmatic processes influence local seismicity and that volcano-tectonic earthquakes have the capacity to change stresses within the shallow and middle crust. These events are large, purely tectonic earthquakes rather than destructive ones; however, their study is important to understand the seismic hazard (Hackett *et al.*, 1996).

STUDY METHODS

Conventional morphologic and structural analyses were performed to identify seismic-related features, assess the influence of tectonically active faults in the landscape, and locate sites for paleoseismic analysis. All these phases were performed with caution because of the ambiguous characteristics of the LATF. We worked with topographic maps (1:50000 scale), aerial photos, and LIDAR images with 5 m-resolution in the ArcMap platform.

Bathymetric, magnetometric and seismo-acoustic surveys were performed inside the LAG crater. We obtained data from twenty-seven bathymetric profiles, seven seismo-acoustic reflection profiles and six magnetometric profiles (lines with NE-SW, N-S and NW-SE orientations). Bathymetry was performed using a Furuno 808 grapher ecosound and a Garmin ecosound GPSMap 325 with a 200 KHz transductor; the seismo-acoustic survey was performed using a sidescan sonar with integrated GPS, fish tow, and 200 KHz transductor; the magnetometry was performed using a portable cesium-vapor magnetometer with integrated Garmin GPS, and Winglink v. 10 software for data corrections.

The paleoseismic study focused on the western segment of the LATF and consisted of a microtopographic survey performed using a Leica precision GPS device and the analysis of three trenches. The microtopography produced a topographic map with 20-cm-interval contour lines used to choose the trench sites. The study of the trenches was performed according to the methodological guidelines detailed in McCalpin (1996).

The first trench or T1 (19°48'25.2" N, 101°27'03.6" W, 2164 m a.s.l.) is a NE-SW-oriented dig in the LAG crater, that exposes the phreatomagmatic sequence deposited in the maar and in the related basement formed by the andesitic lava flow of Cerro Pelón volcano (Figure 3). Trenches T2 and T3 were excavated in the fault scarp and were north-south-oriented, but only T2 (19°48'14.6" N, 101°27'50.4" W, 2118 m a.s.l.) allowed to observe the fault and affected soils. Details of trenches T1 and T2 will be discussed in the results section.

A pedological analysis was carried out at the Laboratorio de Suelos of the Universidad Michoacana de San Nicolás de Hidalgo since the LATF displaces recent soils. Three sites were chosen for soil profiling: one inside trench T2, and the other two 10 m away from the trench, in the hanging wall and in the footwall, respectively. The materials were characterized physically and chemically, and classified according to the Food and Agriculture Organization (FAO) guidelines for genetic soil horizon interpretation and diagnosis (Jahn *et al.,* 2006). Only three samples from sediments and soil material exposed in T2 were selected and dated since most of the area lacks of datable material. The samples ages were obtained with accelerator mass spectrometry (AMS) radiocarbon by BETA Analytic Laboratories. The ages were calibrated with the IntCal13 curves (Table 1).

Table 1. Radiocarbon ages measured for organic sediments from trench T2 following AMS technique. Results were provided by Beta Analytic Inc. The calibrated ages have been obtained using 2σ uncertainty, and the IntCal13 curves (Reimer *et al.*, 2013).

Sample name (unit)	Type of sample	Measured age (years BP)	C^{13}/C^{12}	Conventional age	Calibrated age (years BC/BP)
C1 (Unit 4c)	Soil (bulk)	19160 ± 70	-17.2 0/00	19290 ± 70 BP	21485–21085 BC 23435–23035 BP
S1 (Primary soil: Unit 4b filling A1 fault)	Soil (bulk)	17310 ± 60	-16.6 0/00	17450 ± 60 BP	19290–18950 BC 21240–20900 BP
A1 (Secundary soil: U3)	Soil (bulk)	10480 ± 40	-18.5 0/00	10590 ± 40 BP	10710–10575 BC 12660–12525 BP 10515–10485 BC 12465–12435 BP

RESULTS AND DISCUSSIONS

Geomorphology

The morphological analysis of the study area shows volcano-tectonic and seismotectonic landforms that match with the Dramis and Blumetti classification (2005). The formation of straight and steep scarps, counter-slopes in El Picacho volcano and small graben-horst features were related to tectonic stress (seismic/volcanic). According to Blumetti *et al.* (2002), these landforms are indicators of extensional environments. Other landforms in the area such as deviation of the drainage network, decapitated channels, alignment of monogenetic cones, and *en échelon* faults indicate a minor left-lateral displacement, according to Keller and Pinter (1996).

Similar seismotectonic landforms are reported in other areas of the MAFS (Ramírez-Herrera, 1998), such as the displacement of the southern flank of the Amealco Caldera (Aguirre-Díaz and Mc Dowell, 2000), the graben in the Temascalcingo volcano (Roldán-Quintana *et al.,* 2011; Sunye-Puchol *et al.,* 2015), the *en échelon* geometry of Los Azufres faults, the collapse of El Estribo volcano (Pola *et al.,* 2014) and the uplift of lacustrine sequences in Pátzcuaro lake (Israde-Alcántara *et al.,* 2005; Garduño-Monroy *et al.,* 2009).

Bathymetry and magnetometry

The bathymetry shows a maximum depth of 11 m in the lake of the LAG maar; the profiles allow to trace the LATF underwater and visualize its vertical displacement on the lake floor (Figure 4 profile A, B). The vertical displacement was quantified from the sonograms, which record a vertical displacement of ~50 cm on the fault trace (Figure 4 profiles C, D). These profiles also differentiate four sedimentary units (U1-U4, Figure 4), and allow to delimit the diatreme geometry. Finally, the magnetometric survey shows a N84°oriented diatreme (volcanic neck), matching the superficial LATF trace (Figure 4).

Structural analysis

Three fault systems with ENE-WSW, NW-SE and NE-SW trends are found in the study area. The interaction between those systems creates conspicuous *en échelon* geometries and pull-apart structures. We identified eight regional faults with ENE-WSW trend, belonging to the MAFS. All of the faults develop scarps with heights between 20 and 100 m, but only 25 % of them cause deviations in the drainage network (Supplementary Table 1, Figure 2).

In this study, a minor, left-lateral displacement of the ENE-WSW-trending faults was defined, with a striation measurement at the LATF plane (N80°E/76°NW dip, 60° rake) and the geomorphological features previously described. According to Pérez-Orozco *et al.* (2018), in this area, the ENE-WSW-trending faults present normal displacements with a minor left-lateral component, as the result of a NW-SE extension. In Mennella (2011), the NE-SW and NW-SE-trending faults exhibit normal displacements with minor left-, and right-lateral components, and seem to be reactivated by the movement of the ENE-WSW-trending faults.

The stress distribution in the zone shows that σ_3 is oriented NW-SE, σ_2 is oriented in NE-SW direction, and σ_1 is in vertical position, slightly displaced towards the horizontal (Figure 2b). Similar stress distribution was found in the Acambay-Tixmadejé fault (Martínez-Reyes and Nieto-Samaniego, 1990; García–Palomo *et al.,* 2000; Suter *et al.,* 2001; Quintero-Legorreta, 2002).

Paleoseismic analysis

This section details the characteristics of the first (T1) and second (T2) trenches, where the faulting seems better preserved. Both sites expose the phreatomagmatic sequence deposited during the emplacement of the LAG maar. The sequence is composed of an alternation of four types of deposits: 1) a stratified ash fall layer, 2) a fine ash layer with formation of accretionary lapilli, 3) a discontinuous, wedged gravel layer, and 4) a massive, poorly sorted, grain-supported deposit, composed of sub-angular boulder-to gravel-size lithics. Ballistic impact structures and crossed stratification structures were also observed (Figure 3).

T1 trench

T1 (21 m long and 3 m high) is located in the eastern flank of the LAG crater (Figure 2c), and exposes the phreatomagmatic sequence affected by normal faults and conjugated fractures with NNW-SSE, NW-SE and E-W trends (Figure 5). These faults were classified in main faults (first-order structures) and small-scale faults (second-, third- and fourth-order structures) according to their size and the number of stratigraphic units affected (Supplementary Table 2). T1 shows a graben-horst-graben geometry, limited by the first-order structures, identified as F1, F2, F3, F4, F5, and F6 (Figure 5b, 5c). F1 (N67°W-53°SW) is the main fault exposed in the trench; we measured the vertical displacement on its plane. However, the total displacement in the trench could not be calculated because of the lack of correlative beds across the outcrop and the geometry of the wedged strata.

The first graben (*graben a*) is delimited by F1, F2 (N23°W-83°SW), and F3 (N10°W-84°SW). In F1 we measured two displacements: at the top, a 92 cm-displacement of an alternated sequence of coarse ash layers with accretionary lapilli and gravel strata; at the bottom, a 107 cm-displacement of a lithified, fine ash layer (green and yellow layers in Figure 5a, respectively). The differential displacement indicates that, at least, two rupture events occurred on the F1 fault plane. F1 and the space between F2 and F3 are filled with a mix of phreatomagmatic materials, soil, and imbricated rocks with diameters between 10 and 20 cm.

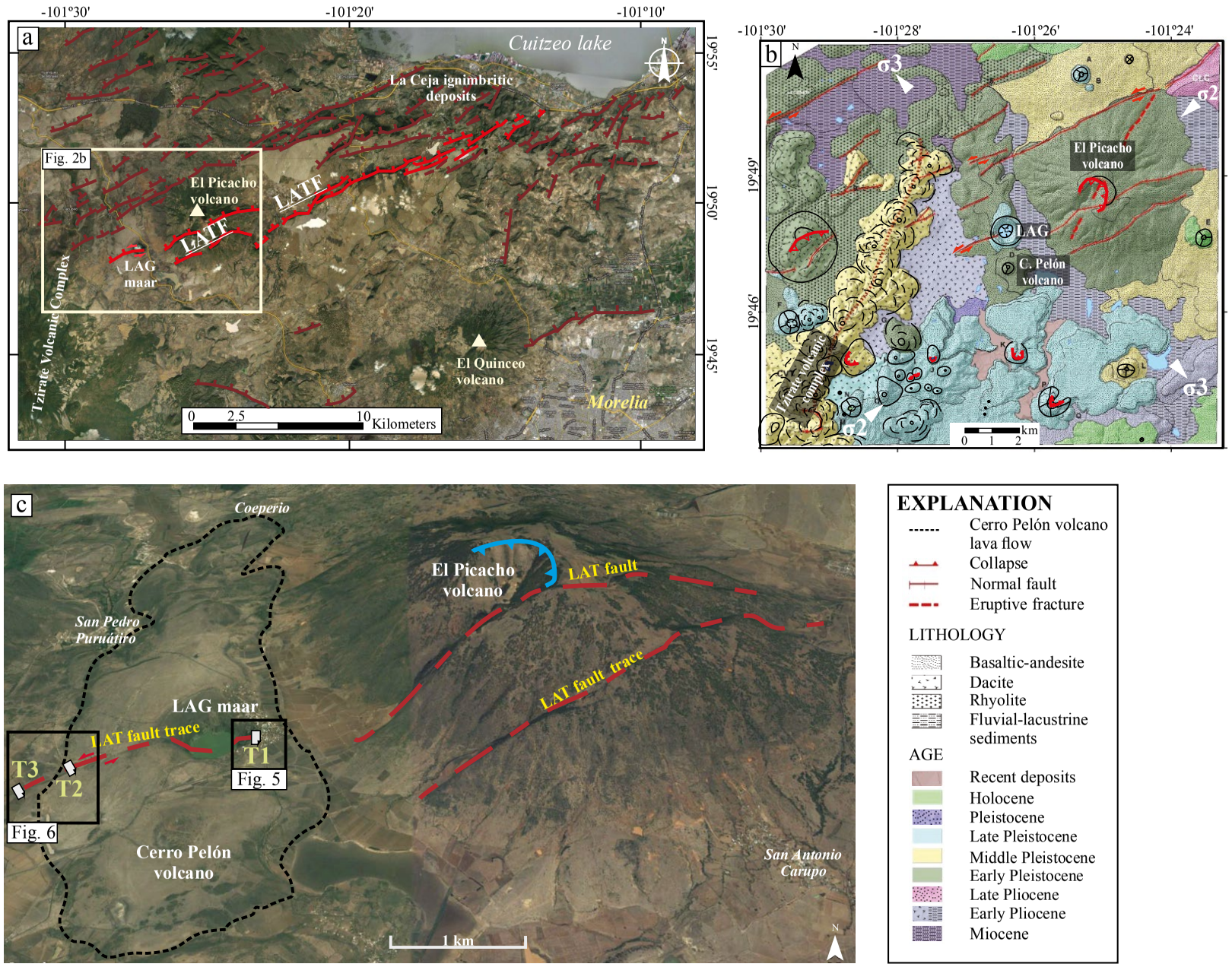

Figure 2. a) Location of the La Alberca-Teremendo fault (LATF) showing the complex geometric array. b) Local geology of the study area, main structures and stress field. c) Aerial view of the trenched area. The dotted line indicates the limit of the basaltic-andesitic lava flows from the Cerro Pelón volcano which underlay the La Alberca de Guadalupe maar (LAG). View of the collapsed summit of El Picacho volcano.

The horst is delimited by F3 and F4 (N83°W-62°SW). The latter is filled with a mix of phreatomagmatic materials and soil; the vertical displacement measured on F4 was 123 cm of a layer of fine ash with accretionary lapilli (brown layer in Figure 5a). Finally, the second graben (*graben c*) is delimited by F4, F5 (N08°W-75°E), and F6 (N39°W-61°NE); F5 is filled with phreatomagmatic materials mixed with soil; the displacement measured on F6 was 20 cm of a gravel layer overlaid by lithified ash strata (purple layer in Figure 5a).

The small-scale faults (second-, third-, and fourth-order structures) are more abundant in the horst, followed by *graben c*, and less abundant in *graben a*; they create small-scale graben, semi-graben and horst geometries, and also merge forming faults nets. These structures do not show vertical displacement across the grabens, and the third-, and fourth-order structures disappear, both, upwards and downwards in the sequence. These characteristics suggest accommodation of materials due to horizontal extension of non-tectonic nature; accordingly, they cannot be used in the paleoseismic estimations.

T2 Trench

T2 trench (10 m long and 4.5 m deep) is located at the western end of the LATF (Figure 2c and Figure 6). The trench exposes the phreatomagmatic sequence of the LAG maar covered by two dark brown, superposed soils with thicknesses between 0.5 and 1.5 m. The soils characteristics are described in detail in the next section.

T2 shows the LATF trace and three smaller antithetic faults (A1-2-3, Figure 7), as well as second- and third-order faults and associated fractures, which displace the phreatomagmatic sequence. The LATF is a normal fault trending N260° and 76°NW dip; at the bottom, it changes to vertical, and at the top has an 89° dip, and a 60° rake. It has a total vertical displacement of 335 cm and a net vertical displacement of 262 cm. The antithetic faults that limit the blocks were identified as A1 (N60°E-80°SE), A2 (N80°E-60°SE) and A3 (N85°W-80°SW). These faults accumulate a vertical displacement of 73 cm (10 cm for A1, 57 cm for A2, and 6 cm for A3). The hanging wall shows a domino-style, normal faulting, integrated by three blocks which rotate 8° to 15° away

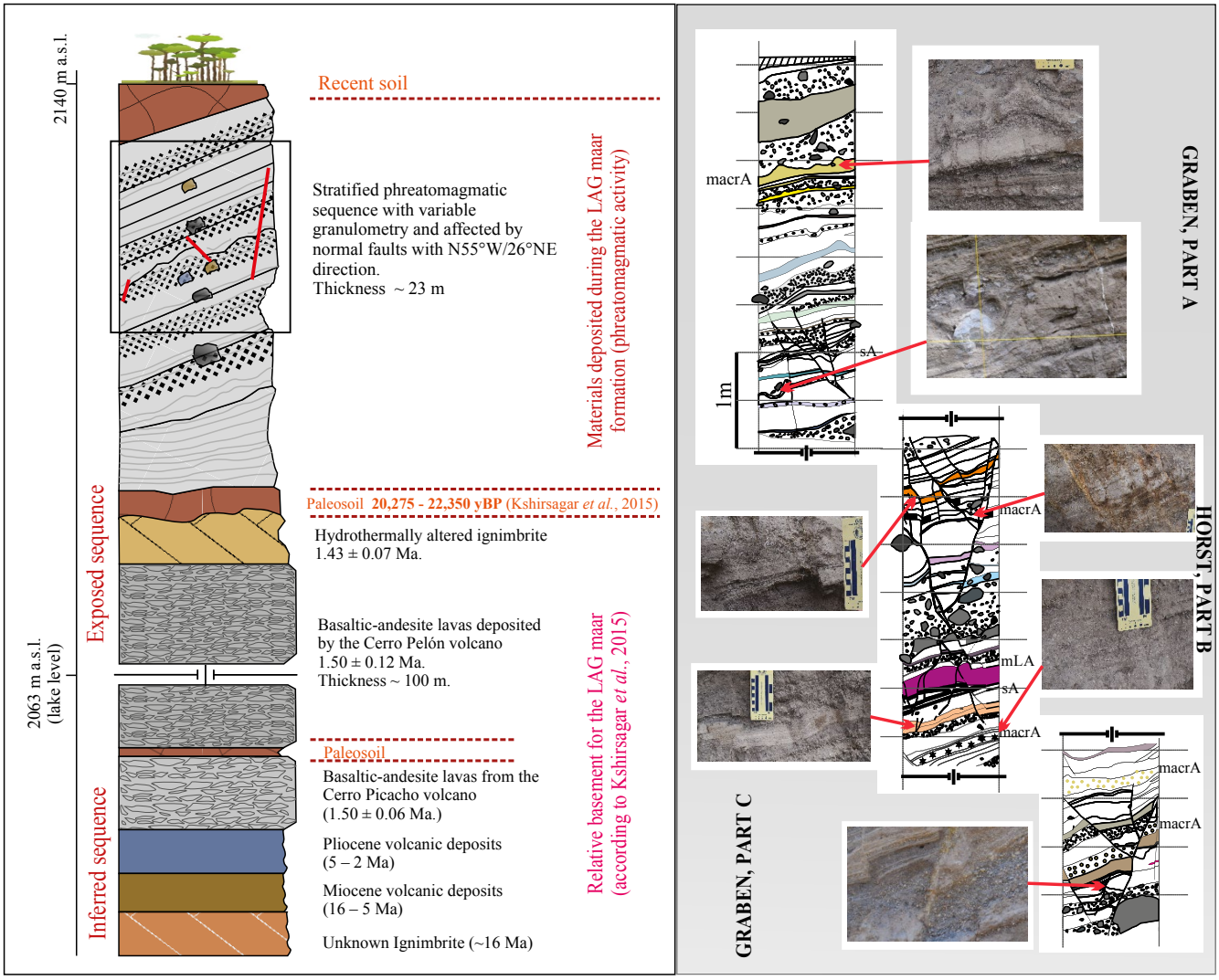

Figure 3. Left: Simplified stratigraphic sequence of the volcanic deposits in the area of the La Alberca de Guadalupe (LAG) maar (Not to scale). The inferred sequence and the dates are by Kshirsagar *et al.* (2015). Right: Details of the faulted phreatomagmatic sequence and photographic record of its structures: folding, andesitic lithic and impact sag, small scale graben-horst geometry, cross-stratification, accretionary lapilli with diameters between 0.2 and 1.5 cm, micro-faulting and ash deformation, and fault affecting material of varied granulometry (thick lapilli to fine ashes). Abbreviations: macrA = masive layer of ash with accretionary lapilli; sA = Stratified, fine ash layer; mLA = massive, fine ash layer.

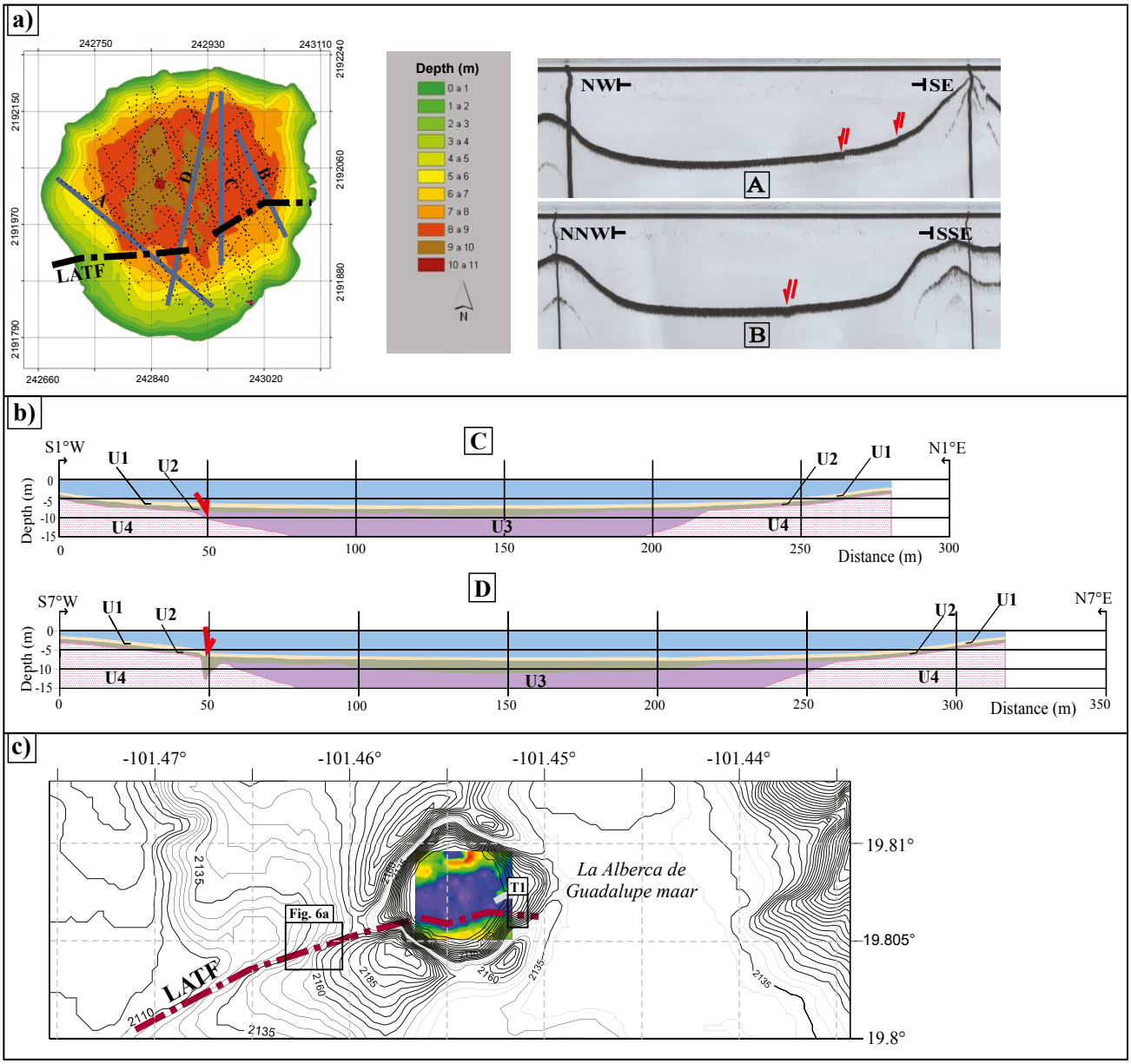

Figure 4. a) Bathymetric map and localization of acoustic profiles through the lake of the LAG maar. Profiles A and B record displacement in the lacustrine floor, the arrows indicate anomalies. b) Sonograms of profiles C and D showing different sedimentary units and displacements in the lacustrine floor. c) Topographic map combined with the reduction-to-the-pole regional magnetic data map (colors). The dotted line indicates the La Alberca - Teremendo fault trace.

from the foot wall; the spaces between blocks (4 to 61 cm) are filled with a mix of phreatomagmatic materials and soil (Figure 7).

Use of soil analysis as a tool for the identification of paleoearthquakes

The soils analyzed in the study area (hanging wall and footwall) were classified as a Luvisol with well-developed A and B horizons, formed from the phreatomagmatic materials with andesitic composition. The on-fault exposed soil (T2 trench) shows variations in its physicochemical properties: the bottom was classified as Luvisol, but at the top, the vertic properties become important, suggesting an evolution towards a Vertisol (Supplementary Table 3). The main variations in the soil exposed on T2 trench are:

1. A noticeable textural change caused by the increase in percentage of clay at 100 cm- depth (terminus *Abruptic,* Jahn *et al.,* 2006).

2. The presence of a lithological discontinuity at 80 cm-depth caused by an anomalous increase in the percentage of organic material (terminus *Ruptic,* Jahn *et al.,* 2006).

3. The presence of recent sediments, 50-cm thick, deposited over an old soil (terminus *Novic,* Jahn *et al.,* 2006).

The previous characteristics are not related to the andic properties of the soil, but rather suggest a disordered soil, with high rates of skeleton and expansive clay.

The soil profile exposed in T2 can be interpreted as two superimposed soils. At the base is an older, primary soil composed by two horizons 2C, characterized by vertic properties, a clayey texture and the presence of slickensides. This soil lacks horizons A and B, possibly due to increased erosion (Figure 7). According to the radiocarbon dates, the lower limit of this soil has an age of 21240–20900 cal yr. BP.

The primary soil is covered by a secondary soil, made of horizons A1-2, B and C. A1-2 have humified organic matter mixed with altered minerals; horizon B is characterized by argillic properties, accumulation of clay, high expansibility, and slickensides; finally, horizon C has vertic properties, slickensides, and a sandy texture (Figure 7). The radiocarbon age at the base of the soil is 12660–12435 cal yr. BP, and continues its development until today.

The differences between the superimposed soils that evolved at different times, suggest a disruption in the pedogenic evolution of the buried soil. This fact may be related to the vertical displacement of the fault and the subsequent formation of a surface soil with unique characteristics derived of the previous soil as parental material. This new soil was displaced again in recent times. The soils analysis suggests that, at least, two ancient earthquakes in the LATF occurred after the emplacement of the LAG maar.

Number of seismic events

The net vertical displacement measured for the LATF in the fault plane in T2 was of 262 cm (335 cm of total synthetic displacement

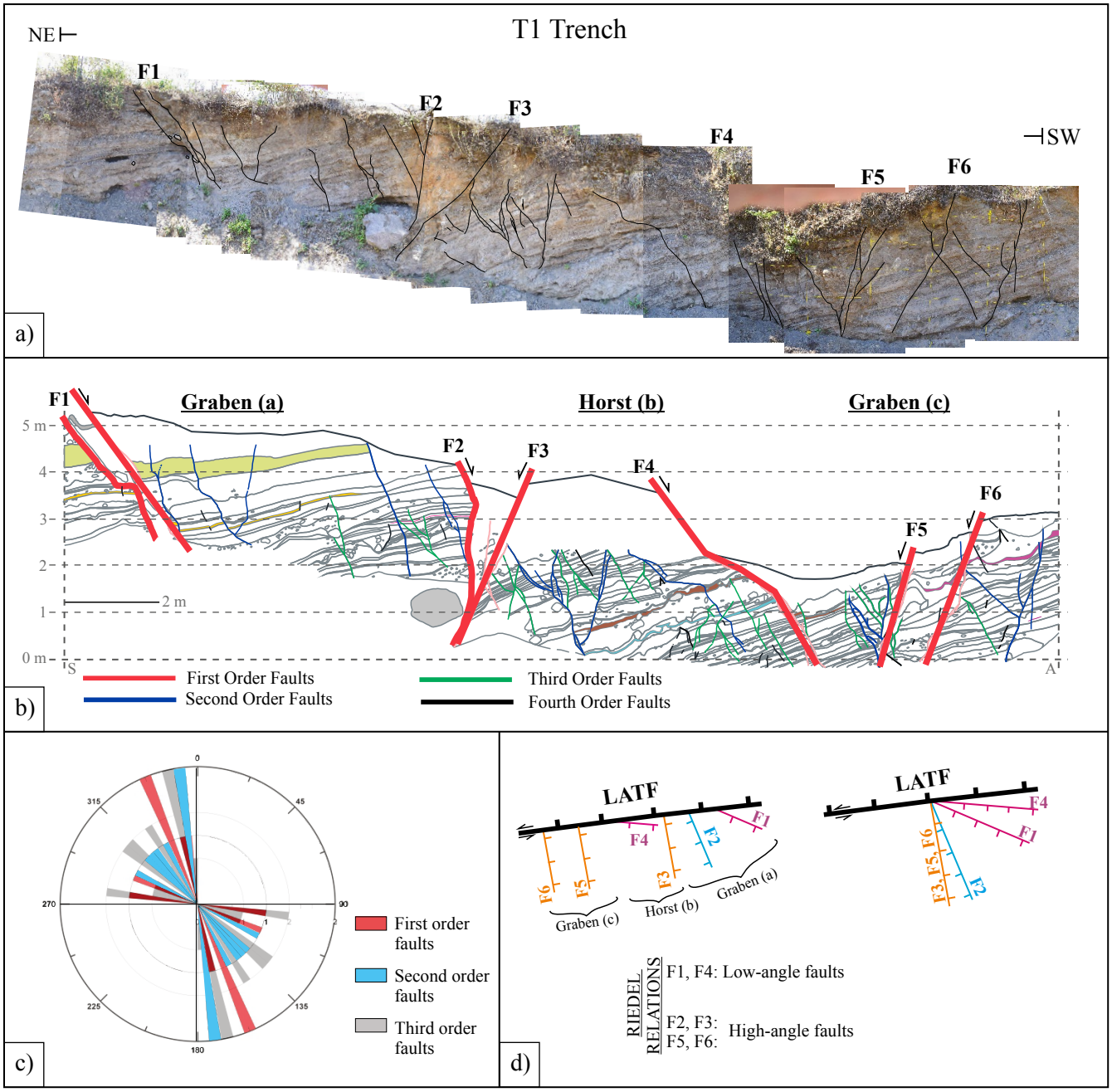

Figure 5. a) Composed photography of the trench T1, an artificial outcrop exposed along the path that connects the crater border with the lake, inside the LAG maar. In the photo, the main faults are delineated. b) Simplified diagram of T1 with the main faults identified (first-, second-, third- and fourth-order). c) Rose diagram of the measured faults indicating a preferential NW-SE strike. d) Sketch map showing the orientation of these outcrop-scale faults with respect to the La Alberca-Teremendo fault and their interpretation as Riedel faults.

Table 2. Slip rates (SR) obtained for partial displacements measured for NW-SE faults in trench T1 and for total and partial displacements of LATF measured in trench T2. Recurrence intervals (RI) obtained for the measured displacements. Ev = Displacement event. (*) = age of the LAG maar from Kshirsagar *et al*., 2015.

	T1 Trench: F1		**T2 Trench: LATF**		**Retrodeformation scenario**		
	Ev 1	Ev2	Complete fault		Ev 1	Ev 2	Ev 3
Total displacement (mm)	920	1070	3350		1130	820	1400
Net displacement (mm)	--	--	2620		880	590	1150
Average vertical displacement (mm)	--	--	Total Net		1117 873		
Time elapsed (years)	*21000		23434-23035		23434-23035	10999 – 10,375	12660 – 12,435
SR (mm/year)	0.046		Total	0.142 – 0.145	0.048 – 0.049	0.074 – 0.079	0.11 – 0.112
			Net	0.112 – 0.114	0.037 – 0.038	0.053 – 0.056	0.09 – 0.092
RI (years)	~11630		Total		7784 ± 81		
			Net		7726 ± 68		

minus 73 cm of total antithetic displacement). We suggest that the observed displacement could be the result of three events: the first could be a volcano-tectonic event related to the LAG maar emplacement; the second event was identified from a net vertical displacement of 59 cm of the buried soil; finally, the third earthquake was identified from a net vertical displacement of 115 cm of the surface soil that likely occurred at prehistoric times. It is clear that the surface soil is displaced and the scarp shows little erosion, but neither historic nor instrumental record exists about this event; therefore, we assigned a maximum age of 1000 yr. BP for this earthquake.

However, estimations should be carefully considered because of the nature of the LATF, and the coexistence of magmatic and tectonic activity in the area.

Deformation model

According to the scenario previously proposed, we defined a model for the reconstruction of the deformation in trench T2 (Figure 8). The first phase is the deposit of the non-deformed, phreatomagmatic sequence during the formation of the La Alberca de Guadalupe maar around 23434–21000 yr. cal BP. The second phase is the occurrence of a volcano-tectonic earthquake related to the formation of the LAG maar around 23434–21000 years ago, causing an 88-cm vertical displacement of the phreatomagmatic sequence and generating a fracture filling of pyroclastic material that resembles a colluvial wedge. This event is followed by a quiescence period (third phase) characterized by the erosion of the upper layers of the phreatomagmatic sequence in the hanging wall (Units 5a-d), and followed by the development of a primary soil (phases fourth and fifth, Units 4a-b, Figure 8). The sixth phase is the occurrence of a tectonic event 12660–12435 years ago, that caused a vertical displacement of 59 cm of the primary soil and the phreatomagmatic sequence. The seventh phase is a quiescence period characterized by the erosion of unit 4a in the hanging wall, followed by the development of a secondary soil from material of the buried soil (eighth phase). Finally, the ninth phase is a third event occurred in recent times, causing a vertical displacement of 115 cm of the newly formed soil. The scarp is still visible today.

Slip Rates (SR)

To measure the slip rate (SR) we followed the methodology used by McCalpin (1996) that considers:

$$SR = \text{Total displacement (mm)}/\text{time elapsed (years)} \qquad \text{(Eq. 1)}$$

The average slip rate was estimated for the net vertical displacement of the LATF (262 cm) measured in T2 and for the displacements of F1 measured in T1 (92 and 107 cm). The slip rates for individual events were estimated but considered with caution because of the lack of datable material in the area (Table 2).

If we assumed a purely tectonic behavior, the average SR obtained for the net vertical displacement of the LATF was 0.114 mm/year, this value represents 23 % of the SR estimated by Suter *et al.* (2001) using geomorphological indicators (0.5 mm/year). The slip rates of individual events show great variation (from 0.037 to 0.141 mm/year) indicating a high degree of uncertainty, consequently, they cannot be used in the evaluation of seismic cycles. The slip rate obtained for the vertical displacements measured in F1 was 0.046 mm/year, but F1 is a secondary fault that could have moved with the volcano-tectonic events of the LATF.

The slip rate values for the LATF are similar to the SR obtained for other faults in the MAFS, especially in the Morelia-Cuitzeo region (0.05 to 0.18 mm/year) (Suter *et al.,* 2001); whereas in the Acambay graben and the Pátzcuaro region, the SR is more variable: 0.03–0.37 mm/year and 0.009–2.78 mm/year, respectively (Suter *et al.,* 1992; Langridge *et al.,* 2000; Garduño-Monroy *et al.,* 2009).

Recurrence intervals

According to McCalpin (1996), the recurrence interval can be assessed with two methods: the direct method and the geological method. The first one produces an average recurrence interval; the second method produces individual recurrence intervals, better reflecting the dynamics of individual faults and their seismic cycles (Scholz, 1990).

For the LATF, we used the direct method to estimate the average recurrence interval for the average vertical displacement considering three displacement events (total = 111.7 and net = 87.3 cm), with the following relation:

$$RI = VDaver / SR - C \qquad \text{(Eq. 2; McCalpin, 1996)}$$

Where VDaver is the average vertical displacement (mm); SR is coseismic slip rate (mm/yr) and C is slip rate per creep. Recurrence intervals for individual events in T2 trench cannot be calculated because of the uncertainty of the associated slip rates. For all the calculations, we assumed that in the LATF, C = 0.

We obtained average recurrence intervals of 7784 ± 81 years for total displacement and 7726 ± 68 for net displacement for the LATF in T2; and an average of 11630 years recurrence interval for F1. These values are closer to the recurrence intervals calculated for other segments of the MAFS such as the Pastores fault (10-15 Ka according to Langridge *et al.,* 2013; Ortuño *et al.*, 2015), and the San Mateo fault (11570 ± 5320 years according to Sunye-Puchol *et al.,* 2015). In the

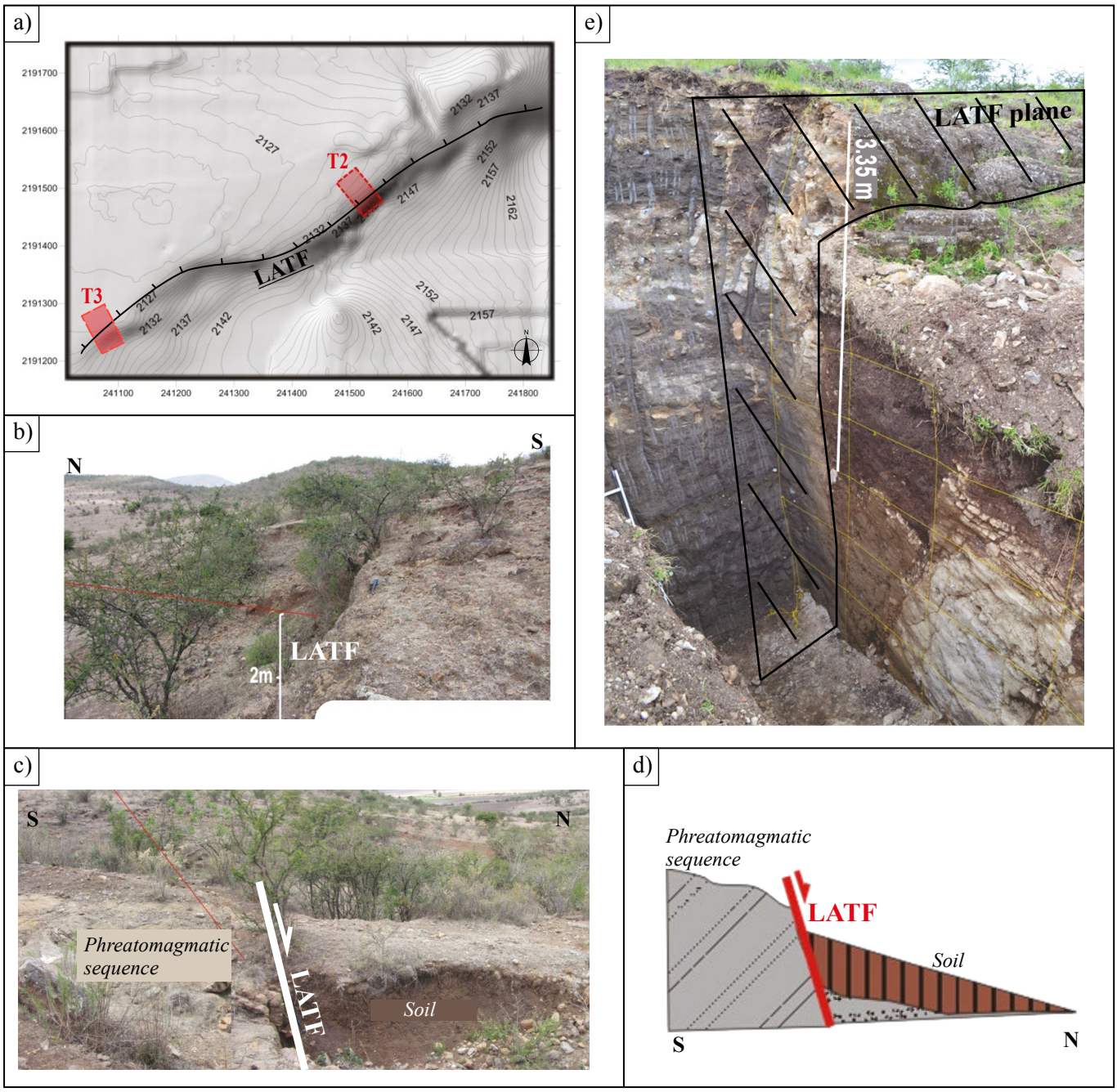

Figure 6. a) Microtopography of the La Alberca-Teremendo fault scarp at the western flank of the LAG maar crater (Equidistance of contour lines: 1 m), and location of trenches T2 and T3. b) Photography of the scarp at the T2 location. c) Photography of the contact between the phreatomagmatic sequence and the soil along the LATF plane. d) Scheme of the photography c). e) Opening of trench T2 with the fault plane exposed.

faults of the Pátzcuaro-Morelia region the values are more variable: our RI is similar to the Huiramba fault, the La Paloma fault, the Charo fault and the Queréndaro-Indaparapeo fault (4.5 to 20 Ka; Garduño-Monroy *et al.,* 2009). These recurrence intervals are a first approach to evaluate the fault activity and should be taken cautiously, as occurrence of strong earthquakes could be clustered in time, with few years and even days of separation, as has been observed elsewhere in the world (Iezzi *et al.,* 2018). We must also consider the frequency of events in the LATF that is influenced by the magmatic activity in the area, which likely changes the fault stresses.

Probable magnitude of individual earthquakes and maximum potential magnitude expected for a seismic rupture in the LATF

The probable magnitude for fault ruptures can be assessed using empirical relations that use fault parameters such as: the surface rupture length, vertical displacement per event, slip rate, and recurrence intervals. Published empirical relations were constructed with global data bases and can be used as reference for sites with scarce or null information. The most used empirical relationships apply the surface rupture length (SRL), but its main uncertainty resides in the lack of information about the geometry and prehistoric length of the faults (Lafuente-Tomás, 2011).

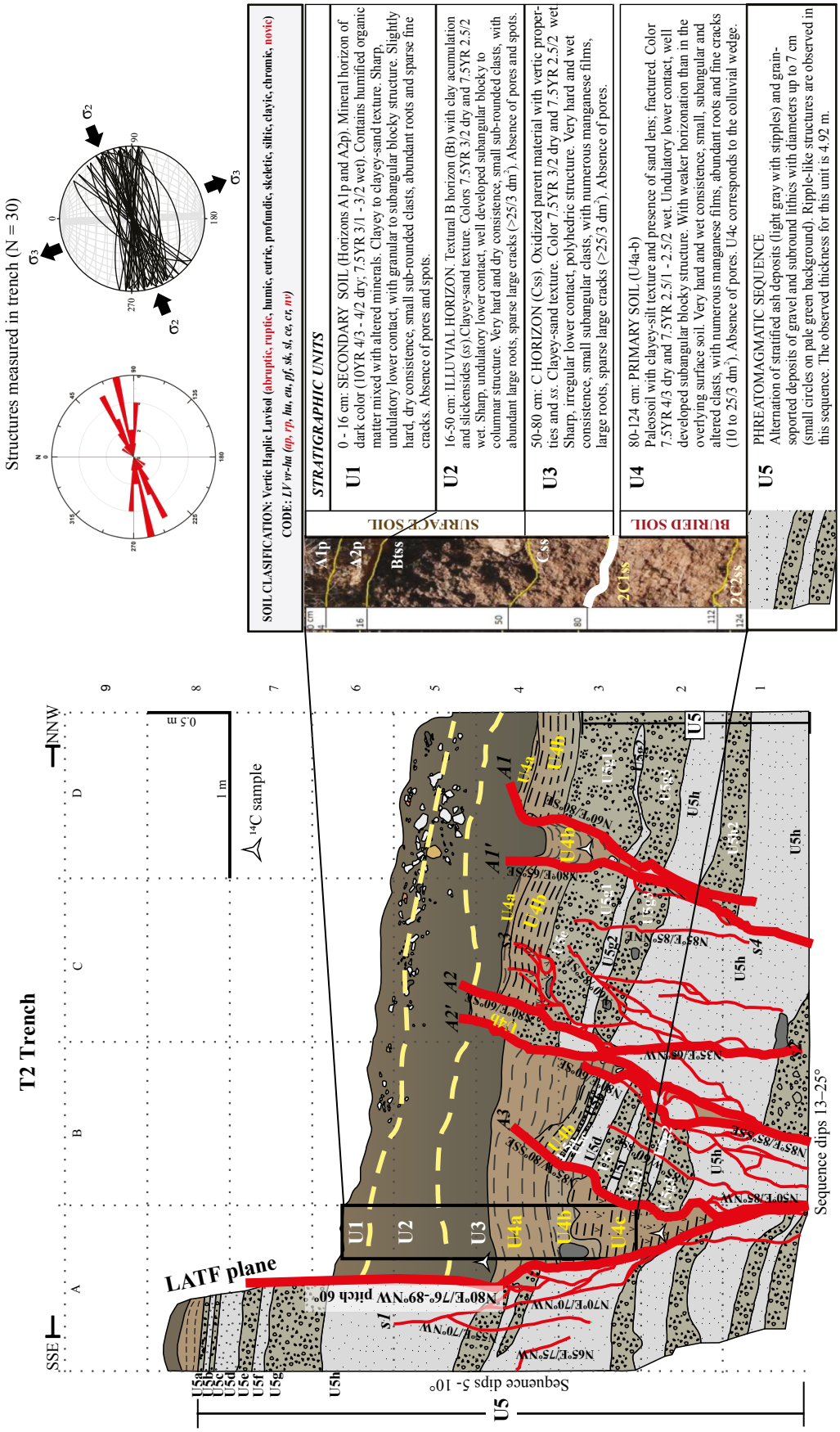

Figure 7. Log of trench T2, rose diagram of the fault planes exposed, directions of the stress field, and pedological analysis and classification of the soil affected by the LATF. Abbreviations: A1-3 = Antithetic faults; s1-5 = second order faults; LATF = La Alberca-Teremendo fault.

Table 3. Resolved scaling relations for assessment of potential Mw magnitude in the displacement events identified in T1 and T2 trenches. The values obtained for the Mohammadioun and Serva (2001) relation are referred as surface wave magnitude (*Ms).* VD = Vertical displacement. SRL = Surface rupture length. Data marked with (*) were obtained from Clemente-Chávez *et al.* (2013) and Singh *et al.* (2011, 2012).

Event	Used relations	Assessed magnitudes (Mw)				
Maximum rupture event for the La Alberca – Teremendo fault (SLR)	Wells and Coppersmith, (1994)	6.72				
	Anderson *et al.,* (1996)	6.77–7.29				
	Stirling *et al.*, (2002)	6.70–7.32				
	Wesnousky (2008)	6.78				
	Mohammadioun and Serva (2001)	5.88 *(Ms)*	using $\Delta\sigma$ = 11.1 bar (*average stress drop for the TMVB)			
		6.69 *(Ms)*	using $\Delta\sigma$ = 50 bar (*minimum stress drop for Morelia region)			
		T1	**T2**			
		F1 Average VD	Average VD	Events		
				Ev 1	Ev 2	Ev 3
Individual net displacements measured for T1 and T2 trenches (VD)	Hanks y Kanamori (1979)	6.5	6.6 – 6.9	6.7	6.6	6.8
	Wells and Coppersmith (1994)	6.6	6.8 – 7.0	6.8	6.6	7.0

The LATF has characteristics that indicate it could move under the influence of both, an extensional volcanic environment and the actual tectonic regime. So, in order to obtain a reliable evaluation of the deformation for this fault, a specific paleoseismic relation should be constructed; however, more information is needed from others structures in this area in order to achieve a reliable relation. We used published relations for the LATF, although we took into consideration that they could produce an overestimation of magnitudes of the paleoseismic events, and magnify the fault seismic potential. We applied relations that include the average vertical displacement (VD) to assess the probable magnitude associated to individual events, and relations that use SRL and SR to estimate the maximum magnitude for an earthquake that displaces the entire fault trace; finally, we made a comparison between relations to establish the best estimation (Supplementary Table 4).

For the LATF (Table 3), if we assume that all the deformation is of tectonic nature and that the segments are connected in depth, the magnitude M_w values based on the total surface rupture length of 26.1 km, ranges between 6.7 and 7.3, and between 5.9 and 6.7 for superficial magnitude (M_S). These values are slightly higher than those obtained for other segments of the MAFS. For example, for the Pastores, Acambay-Tixmadejé, Maravatío, La Paloma, Venta de Bravo, San Mateo faults, values range between 6.4 and 7.0, and for the Pátzcuaro-Morelia faults, the M_w values are 5.8 to 7.1. Meanwhile, for the individual events, the probable magnitude M_w, based on the average slip, ranges between 6.6 and 7.0. Finally, for the slip measured in F1 of T1, the estimated magnitudes range M_w = 6.5–6.6. The similar displacements values of trenches T1 and T2 suggest that the inferred events on the LATF trace influence the fault F1 movement, and the faulting could be simultaneous. The M_w figures obtained using the relations of Anderson *et al*., (1996) and Stirling *et al*., (2002) are higher than those obtained using the relations of Wells and Coppersmith (1994) and Wesnousky (2008), but the minimum magnitude remains around 6.7 for a rupture of 26 km of the LATF.

If we assume a purely tectonic activity, the magnitudes predicted for the LATF are greater than expected, suggesting the possibility of multi-fault ruptures (primary and secondary displacements triggered by other fault ruptures in the area), in a similar scenario to that of the Acambay graben during the 1912 earthquake (Arzate, *et al.,* 2018; Ortuño *et al.*, 2019). We must consider that secondary behavior on a fault system can also be triggered by large volcanic eruptions (as mentioned in Ortuño *et al.*, 2019). For the LATF in particular both triggers are equally probable.

In a different scenario, if we assume that the movement of the LATF is the result of volcano-tectonic events produced by dike-induced structures under an extensional environment, the estimated magnitudes M_w should be in a range of 4.0 to 5.5 (exceptionally up to 6.5, Hackett *et al.,* 1996), as has been observed in others areas of the world (*e.g.* Africa, Iceland and the USA, Hackett *et al.,* 1996). Moderate magnitude events could be the most probable scenario for a displacement of the LATF or the NW-SE associated faults. However, moderate magnitudes events are not harmless; for example, in the Chapala graben, on October 2, 1847, an earthquake (M_I 5.7) caused several human losses and serious damages to the villages of Poncitlán and Ocotlán (Suter, 2017).

Seismic hazard

The favorable orientation of the LATF in relation with the current stress field in central México enhances the probability of a future rupture in the fault. Considering the minimum potential magnitude for a tectonic event on the fault (M_w 5.9), the earthquake would be perceived in a radius of ~ 200 km, where some of the largest cities in the country concentrate almost 43 % of the population. For a volcano-tectonic earthquake (M_w 4–5) the area would be reduced, but it could affect parts of the states of Michoacán, Guanajuato and México (Figure 9a).

According to the Environmental Seismic Intensity scale (ESI-2007, Michetti *et al.,* 2007), the LATF could generate events with intensities from IV to X, characterized by easily observable environmental effects, often permanent and diagnostic, starting from intensity VII. The analysis of environmental effects is recommended in sparsely populated areas, but they are less suitable for intensity assessment than the effects on humans and manmade structures. For such events, the damaged areas could be as large as 1000 km^2 (IX) and 5000 km^2 (X) (Figure 9b). Permanent and temporary effects could appear within these areas. Primary effects could be surface ruptures of kilometric scale, and local uplift and subsidence. Secondary effects could be

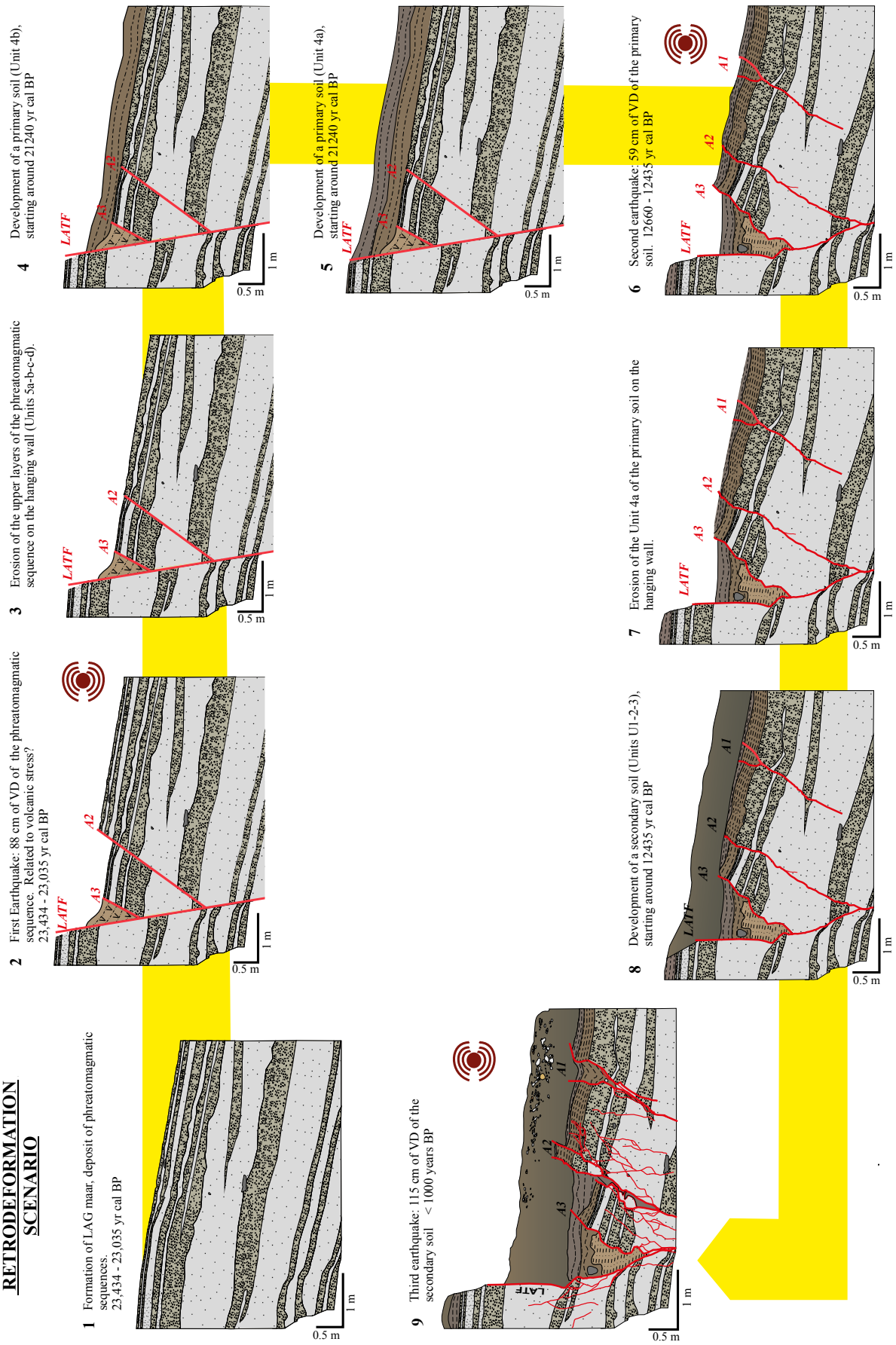

Figure 8. Retrodeformation model for the activity of La Alberca-Teremendo fault (LATF) based on the record from trench T2, indicating the main events (earthquakes) and the current aspect of the trench site. Abbreviations: A1-3 = Antithetic faults; VD = Net vertical displacement; LAG = La Alberca de Guadalupe.

Table 4. Summary of parameters for the paleoseismic analysis in trenches T1 (NW-SE faults) and T2 (La Alberca - Teremendo fault).

Parameter	
Thickness of seismogenic layer	12–20 km (Ortuño *et al.,* 2015)
Crust rigidity	3 x 10^{11} dyn/cm^2
Maximal surface rupture length (SRL_{max}) for LATF	26.176 km
Rupture area (A) for LATF	8.22 km^2
Accumulated maximum throw for LATF	50 m
Partial vertical displacement of F1 fault in T1 (VD_{T1})	92 cm (top) 107 cm (bottom)
Total vertical displacement of LATF in T2 (VD_T)	335 cm
Net vertical displacement of LATF in T2 (VD_N)	262 cm
Total average displacement of LATF in T2 (VD_{averT})	111.7 cm
Net average displacement of LATF in T2 (VD_{averN})	87.3 cm
Individual displacement event 1	113 cm (Total) 88 cm (Net)
Individual displacement event 2	82 cm (Total) 59 cm (Net)
Individual displacement event 3	140 cm (Total) 115 cm (Net)
Elapsed time for displacement of F1 fault in T1	21000 years (Kshirsagar *et al.*, 2015)
Elapsed time for accumulated displacement of LATF in T2	23035–23434 years
Slip rate for F1 fault in T1, (SR_{F1})	0.046 mm/yr.
Average slip rate for VD (SR_{averT}) in T2	0.142–0.145 mm/yr. (Total) 0.112–0.114 mm/yr. (Net)
Recurrence interval obtained for F1 fault in T1	~11630 years
Recurrence interval obtained for LATF in T2	7784 ± 81 years (Total) 7726 ± 68 years (Net)

ground cracks of metric scale, slope movements with bulk volumes of 10^3–10^6 m^3, liquefaction processes, anomalous waves with over 1 m run-up in close basins, temporary spring drying, and streams changes. All these alterations would be particularly important in cities north of Michoacán, such as Morelia, Pátzcuaro, Zacapu, and Cuitzeo, where the granular basement modifies the accelerations of the terrain and can generate liquefaction and infrastructural damage.

CONCLUSIONS

The La Alberca-Teremendo fault (LATF) is a 26 km long, complex, *en échelon* structure, which has normal displacement with a minor left-lateral component. The activity of the LATF is closely linked to the emplacement of the La Alberca de Guadalupe maar and triggered the collapse of the Picacho volcano summit. These volcano-tectonic relationships reflect recurrent fault activity during the Quaternary.

The LATF activity was evaluated in the volcanic phreatomagmatic sequences of the LAG maar. The slip rate of this fault was estimated at 0.114 mm/year with an average recurrence interval of 7726 ± 68 years and an average net vertical displacement of 87.3 cm. Table 4 shows a compilation of the measured parameters in this study.

Paleoseismic analysis suggested that the fault has moved three times in the past 23000 years: the first was a volcano-tectonic event that could be cogenetic to the LAG maar emplacement; we assume a moderate to low magnitude for this event. The other two events were observed more clearly and were related to earthquakes with magnitudes M_w of 6.6–7 if we assumed that they were the result only of tectonic stress.

The two earthquakes were identified through the superposition of two soils observed during the pedological analysis. This study revealed a secondary soil developed from an eroded buried soil, whose evolution was interrupted by the fault activity. The soil analysis provides crucial information for the assessment of the seismogenic potential of the LATF and could be helpful in similar scenarios where faults affect recent soils.

Although the LATF is a complex structure within the MAFS, its seismogenic potential is important because the fault is favorably oriented in relation to the current stress field in central Mexico. Empirical relationships suggest that the fault may generate earthquakes

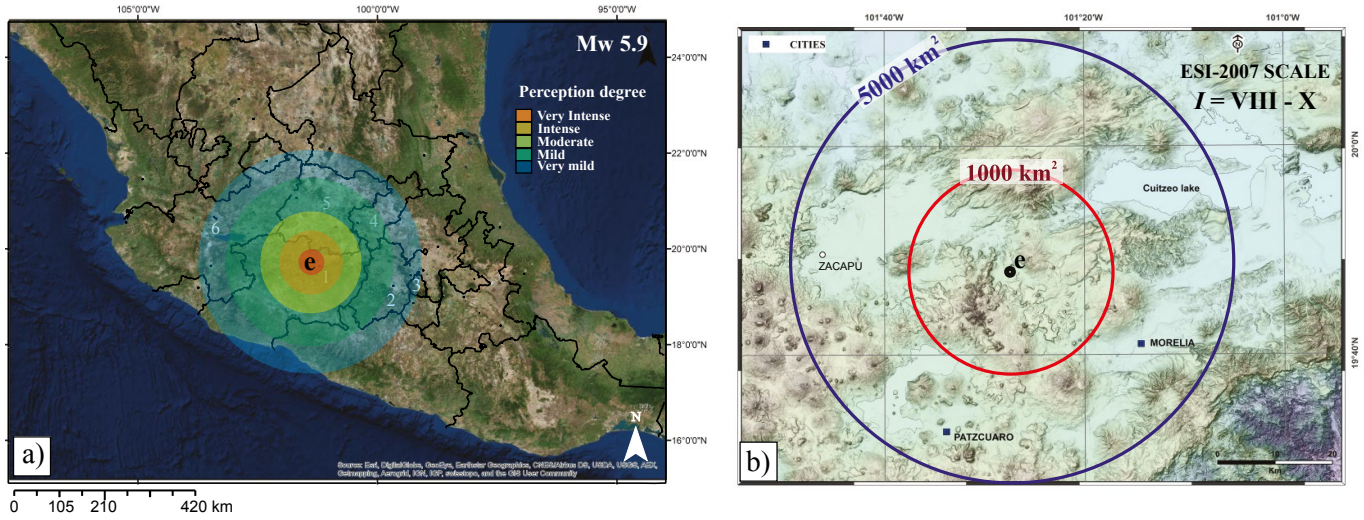

Figure 9. a) Perception area for a moderate event with magnitude Mw 5.9 and epicenter in the La Alberca-Teremendo fault. b) Areas prone to develop environmental effects during an earthquake with intensities between VIII - X (1000 km^2–5000 km^2). Numbers indicate Mexico states: 1 = Michoacán; 2 = Estado de México; 3 = México City; 4 = Querétaro; 5 = Guanajuato; 6 = Jalisco.

with moderate magnitude (4–5) during a volcano-tectonic event, or even with large magnitude (M_w 6–7) during a purely tectonic event.

In Mexico, historical intraplate earthquakes with similar magnitude to that estimated for the LATF have caused severe damages across vast areas, *e.g.* Chapala Graben 1847, M_I 5.7; Acambay 1912, M_w 7; and Axochiapan 2017, M_w 7.1. The effects of these earthquakes were comparable to those produced by the largest subduction seisms in the country, *e.g.* Jalisco 1932, M_w 8.1–8.4; Lázaro Cárdenas 1985, M_w 8 (Singh and Suárez, 1987), and Colima 1995, M_w 8, among others.

Several fault segments with characteristics similar to those of the LATF exist in the western sector of the MAFS, and remain unstudied (for example, Pajacuarán or Ixtlán faults). The proximity of the LATF to some of the largest cities in the country turns it into a seismic source that should be considered in hazard assessment studies and urban planning of Michoacán and central Mexico.

SUPPLEMENTARY MATERIAL

Supplementary Tables 1 to 4 can be found at the journal website <http://rmcg.unam.mx/>, in the table of contents of this issue.

ACKNOWLEDGEMENTS

This study was carried out with the support of a doctoral scholarship No. 59131 granted by the Consejo Nacional de Ciencia y Tecnología (CONACyT) to D.C. Soria-Caballero, the support of project SEP-CONACyT-CB-2009-01-134151 "Estudio tectónico, paleosismológico y arqueosismológico en lagos del Holoceno al Reciente del Cinturón Volcánico Trans-Mexicano y el Bloque Jalisco", and project 17 of Cemie-GEO. The authors thank the careful revisions of Dr. Pierre Lacan, Dr. James McCalpin and an anonymous reviewer, who helped us to improve this work. We are grateful to Dr. Susana Osorio Ocampo and Dr. Gabriela Gómez Vasconcelos for their participation during fieldwork, as well as to Ing. Daniel León from the Departamento de Exploración Sismotectónica y Geofísica of the Comisión Federal de Electricidad (CFE, acronym in Spanish) and Dr. Arturo Chacón from the Instituto de Investigaciones en Recursos Acuáticos (INIRENA, acronym in Spanish) for their participation during the geophysical data acquisition.

REFERENCES

Aguirre-Díaz, G.J., McDowell, F.W., 2000, Volcanic evolution of the Amealco caldera, central Mexico, *in* Delgado-Granados, H., Aguirre-Díaz, G., Stock, J.M. (eds.), Cenozoic Tectonics and Volcanism of Mexico: Boulder Colorado, Geological Society of America Special Paper, 334, 179-193.

Anderson, J.G., Wesnousky, S.G., Stirling, M., 1996, Earthquake size as a function of fault slip rate: Bulletin of the Seismological Society of America, 86, 683-690.

Arce, J.L., Macías, J.L., Rangel, E., Layer, P., Garduño-Monroy, V.H., Saucedo, R., García, F., Castro, R., Pérez-Esquivias, H., 2012, Late Pleistocene rhyolitic explosive volcanism at Los Azufres Volcanic Field, central Mexico, *in* Aranda-Gómez, J.J., Tolson, G., Molina-Garza, R.S., (eds.), The Southern Cordillera and Beyond: Geological Society of America Field Guide 25, 45-82, DOI:10.1130/2012.0025(04).

Arreola, R., 1985, Obras completas de D. Melchor Ocampo, V. 1, La obra científica y literaria: Morelia, Michoacán, México, Comité Editorial del Gobierno del Estado de Michoacán, 510 pp.

Arzate, J., Lacan, P., Corbo-Camargo, F., Arango-Galván, C., Félix-Maldonado, R., Pacheco, J., León-Loya, R., 2018, Crustal structure of the eastern Acambay Graben, Central Mexico, from integrated geophysical data: Revista Mexicana de Ciencias Geológicas, 35(3), 228-239, DOI: 10.22201/cgeo.20072902e.2018.3.864.

Astíz-Delgado, L.M., 1980, Sismicidad en Acambay, Estado de México. El temblor del 22 de febrero de 1979: Ciudad de México, México, Universidad Nacional Autónoma de México, tesis profesional, 130 pp.

Bárcena, M., 1875, Los terremotos de Jalisco: Ciudad de México, México, Boletín de la Sociedad Mexicana de Geografía y Estadística, 2, 240-248.

Blumetti, A.M., Esposito, E., Ferreli, L., Michetti, A. M., Porfido, L., Serva, L., Vittori, E., 2002, New data and reinterpretation on the November 23, 1980, M 6.9 Irpinia–Lucania earthquake (Southern Apennines), coseismic surface effects, *in* Dramis, F., Farabollini, P., Molin, P. (eds.), Proceedings of the Workshop Large Scale Vertical Movements and Related Gravitational Processes: Studi Geologici Camerti, Special Number, 19-27.

Clemente-Chávez, A., Figueroa-Soto, A., Zúñiga, F.R., Arroyo, M., Montiel, M., Chávez, O., 2013, Seismicity at the northeast edge of the Mexican Volcanic Belt (MVB) and activation of an undocumented fault: the Peñamiller sequence of 2010–2011, Querétaro, Mexico: Natural Hazards and Earth System Sciences, 13(10), 2521-2531.

Demant, A., 1978, Características del Eje Neovolcánico Tansmexicano y sus problemas de interpretación: Revista Instituto de Geología, 2(2), 172-187.

Dobson, P.F., Mahood, G.A., 1985, Volcanic stratigraphy of the Los Azufres geothermal area, Mexico: Journal of Volcanology and Geothermal Research, 25, 273-287.

Dramis, F., Blumetti, A.M., 2005, Some considerations concerning seismic geomorphology and Paleoseismology: Tectonophysics, 408, 177-191.

Ego, F., Ansan, V., 2002, Why is the Central Trans-Mexican Volcanic Belt (102°–99° W) in transtensive deformation?: Tectonophysics, 359, 189-208.

Ferrari, L., Orozco-Esquivel, T., Manea, V., Manea, M., 2012, The dynamic history of the Trans-Mexican Volcanic Belt and the Mexico subduction zone: Tectonophysics, 522, 122-149, DOI: 10.1016/j.tecto.2011.09.018.

Flores, T., Camacho, H., Muñoz-Lumbier, M., 1922, Memoria relativa al terremoto mexicano del 3 de enero de 1920: México, D.F., Secretaría de Industria, Comercio y Trabajo, Instituto Geológico de México, Boletín No. 38, 107 pp.

García-Palomo, A., Macías, J.L., Garduño, V.H., 2000, Miocene to Recent structural evolution of the Nevado de Toluca volcano region, central Mexico: Tectonophysics, 318(1), 281-302.

Garduño-Monroy, V.H., 1999, El vulcanismo del Mioceno-Pliocuaternario de Michoacán, *in* Garduño Monroy, V.H., Corona Chávez, P., Israde Alcántara, I., Menella, L., Arreygue, E., Bigioggero, B., Chiesa, S. (eds.), Carta Geológica de Michoacán, escala 1:250 000: Morelia, Michoacán, Universidad Michoacana de San Nicolás de Hidalgo, 27-45.

Garduño-Monroy, V.H., Gutiérrez-Negrín, L.C.A., 1992, Magmatismo, hiatus y tectonismo de la Sierra Madre Occidental y del Cinturón Volcánico Mexicano: Geofísica Internacional, 31(4), 417-429.

Garduño-Monroy, V.H., Pérez-López, R., Israde-Alcántara, I., Rodríguez-Pascua, M.A., Szynkaruk, E., Hernández-Madrigal, V.M., García-Zepeda, M.L., Corona-Chávez, P., Ostroumov, M., Medina-Vega, V.H., García-Estrada, G., Carranza, O., López-Granados, E., Mora Chaparro, J. C., 2009, Paleoseismology of the southwestern Morelia-Acambay fault system, central Mexico: Geofísica internacional, 48(3), 319-335.

Gómez-Tuena, A., Orozco-Esquivel, M. T., Ferrari, L., 2005, Petrogénesis ígnea de la faja volcánica transmexicana: Boletín de la Sociedad Geológica Mexicana, 57(3), 227-283.

Gómez-Vasconcelos, M.G., Garduño-Monroy, V.H., Macías, J.L., Layer, P.W., Benowitz, J.A., 2015, The Sierra de Mil Cumbres, Michoacán, México: Transitional volcanism between the Sierra Madre Occidental and the Trans-Mexican Volcanic Belt: Journal of Volcanology and Geothermal Research, 301, 128-147.

Gómez-Vasconcelos, M.G., Avellán, D.R., Cisneros, G., Macías Vázquez, J.L., Mendiola López I.F., Sosa-Ceballos, G., Layer, P.W., Benowitz, J., Perton, M., 2018, El alineamiento de 13 conos de escoria a lo largo del segmento de falla Queréndaro-Indaparapeo al este del Campo Volcánico Michoacán-Guanajuato: GEOS, 38(1), 158.

Hackett, W.R., Jackson S.M., Smith, R.P., 1996, Paleoseismology of Volcanic Environments, *in* McCalpin, J. (ed.), Paleoseismology: Academic Press, San Diego, California, 147-181.

Hanks, T.C., Kanamori, H., 1979, A moment magnitude scale: Journal of Geophysical Research, 84(B5), 2348-2350.

Hasenaka, T., Carmichael, I.S.E., 1985, The Cinder Cones of Michoacán – Guanajuato, central Mexico: their age, volume and distribution, and magma discharge rate: Journal of Volcanology and Geothermal Research, 25(1-2), 105-124.

Iezzi, F., Mildon, Z., Walker, J.F., Roberts, G., Goodall, H., Wilkinson, M., Robertson, J., 2018, Coseismic throw variation across along-strike bends on active normal faults: Implications for displacement *versus* length scaling of earthquake ruptures: Journal of Geophysical Research, Solid Earth, 123(11), 9817-9841.

Iglesias, M., Bárcena, M., Matute, J.I., 1877, Informe sobre los temblores de Jalisco y la erupción del volcán "Ceboruco" presentado al Ministerio de Fomento por la Comisión Científica que suscribe: Anales del Ministerio de Fomento, 1, 115-204.

Israde-Alcántara, I., Garduño-Monroy, V.H., Fisher, C.T., Pollard, H.P., Rodríguez-Pascua, M.A., 2005, Lake level change, climate, and the impact of natural events: the role of seismic and volcanic events in the formation of the Lake Pátzcuaro Basin, Michoacán, Mexico: Quaternary International, 135(1), 35-46.

Israde-Alcántara, I., Velázquez-Durán, R., Lozano-García, M., Bischoff, J., Domínguez-Vázquez, G., Garduño-Monroy, V.H., 2010, Evolución paleolimnológica del Lago Cuitzeo, Michoacán durante el Pleistoceno-Holoceno: Boletín de la Sociedad Geológica Mexicana, 62(3), 345-357.

Jahn, R., Blume, H.P., Asio, V.B., Spaargaren, O., Schad, P., 2006, Guidelines for soil description, 4th edition: Rome, Italy, FAO (Food and Agriculture Organization), 97 pp, ISBN 9251055211–97.

Johnson, C.A., Harrison, C.G.A., 1990, Neotectonics in central Mexico: Physics of the Earth and Planetary Interiors, 64(2-4), 187-210.

Keller, E.A., Pinter, N., 1996, Active tectonics; earthquakes, uplift, and landscape: Upper Seddle River, New Jersey, USA, Prentice Hall, 338 pp.

Kshirsagar, P., Siebe, C., Guilbaud, M.N., Salinas, S., Layer, P.W., 2015, Late Pleistocene Alberca de Guadalupe maar volcano (Zacapu basin, Michoacán): Stratigraphy, tectonic setting, and paleo-hydrogeological environment: Journal of Volcanology and Geothermal Research, 304, 214-236.

Lacan, P., Ortuño, M., Audin, L., Perea, H., Baize, S., Aguirre-Díaz, G., Zúñiga, F.R., 2018, Sedimentary evidence of historical and prehistorical earthquakes along the Venta de Bravo Fault System, Acambay Graben (Central Mexico): Sedimentary Geology, 365, 62-77.

Lafuente-Tomás, P., 2011, Tectónica activa y paleosismicidad de la falla de Concud (Cordillera Ibérica central): Zaragoza, España, Universidad de Zaragoza, tesis doctoral, 274 pp.

Langridge, R.M., Weldon II, R.J., Moya, J.C., Suárez, G., 2000, Paleoseismology of the 1912 Acambay earthquake and the Acambay-Tixmadejé Fault, Trans-Mexican Volcanic Belt: Journal of Geophysical Research, Solid Earth (1978–2012), 105(B2), 3019-3037.

Langridge, R.M., Persaud, M., Zúñiga, F.R., Aguirre-Díaz, G.J., Villamor, P., Lacan, P., 2013, Preliminary paleoseismic results from the Pastores fault and its role in the seismic hazard of the Acambay graben, Trans-Mexican Volcanic Belt, Mexico: Revista Mexicana de Ciencias Geológicas, 30(3), 463-481.

Martínez-Reyes, J., Nieto–Samaniego, A.F., 1990, Efectos Geológicos de la Tectónica Reciente en la Parte Central de México: Revista Mexicana de Ciencias Geológicas, 9(1), 33-50.

McCalpin, J.P., 1996, Paleoseismology: San Diego, California, Academic Press, 588 pp.

Mennella, L., 2011, Sismotectónica del sector occidental del Sistema Morelia-Acambay, México, a partir del análisis de poblaciones de fallas: Morelia, Michoacán, Universidad Michoacana de San Nicolás de Hidalgo, tesis de maestría, 151 pp.

Michetti, A.M., Esposito, E., Guerrieri, L., Porfido, S., Serva, L., Tatevossian, R., Vittori, E., Audemard, F., Azuma, T., Clague, J., Comerci, V., Gürpinar, A., McCalpin, J., Mohammadioun, B., Mörner, N.A., Ota, Y., Roghozine, E., 2007, Intensity Scale ESI-2007, *in* Guerrieri, L., Vittori, E. (eds.), Memorie Descriptive Della Carta Geologica D'Italia, 74: Rome, Italy, Servizio Geologico d'Italia. APAT, 11–20.

Mohammadioun, B., Serva, L., 2001, Stress drop, slip type, earthquake magnitude, and seismic hazard: Bulletin of the Seismological Society of America, 91(4), 694-707.

Mooser, F., 1972, The Mexican Volcanic Belt: Structure and tectonics: Geofísica Internacional, 12(2), 55-70.

Ortuño, M., Zúñiga, F.R., Aguirre-Díaz, G.J., Carreón-Freyre, D., Cerca, M., Roverato, M., 2015, Holocene paleo-earthquakes recorded at the transfer zone of two major faults: The Pastores and Venta de Bravo faults (Trans-Mexican Volcanic Belt): Geosphere, 11(1), 160-184, DOI: 10.1130/GES01071.1.

Ortuño, M., Corominas, O., Villamor, P., Zúñiga, R.F., Lacan, P., Aguirre-Díaz, G., Perea, H., Štěpančíková, P., Ramírez-Herrera, M.T., 2019, Evidence of recent ruptures in the central faults of the Acambay Graben (central Mexico): Geomorphology, 326, 17-37, DOI: 10.1016/j.geomorph.2018.07.010.

Pasquarè, G., Ferrari, L., Garduño, V.H., Tibaldi, A., Vezzoli, L., 1991, Geological map of the central sector of Mexican Volcanic Belt, States of Guanajuato and Michoacán: Geological Society of America Map and Chart series, MCH 072, 20 pp.

Pérez-Orozco, J.D., Sosa-Ceballos, G., Garduño-Monroy, V.H., Avellán, D.R., 2018, Felsic-intermediate magmatism and brittle deformation in Sierra del Tzirate (Michoacán-Guanajuato Volcanic Field): Journal of South American Earth Sciences, 85, 81-96.

Pola, A., Macías, J.L., Osorio-Ocampo, S., Garduño-Monroy, V.H., Melchor, C.S., Martínez-Martínez, J., 2014, Geological Setting, Volcanic Stratigraphy, and Flank Failure of the El Estribo Volcano, Pátzcuaro (Michoacán, Mexico), *in* STRATI 2013: Springer International Publishing, 1251-1256.

Quintanar L., Rodríguez-González, M., Campos-Enríquez, O., 2004, A shallow crustal earthquake doublet from the Tran-Mexican Volcanic Belt (Central Mexico): Bulletin of the Seismological Society of America, 94, 845-855.

Quintero-Legorreta, O., 2002, Análisis estructural de fallas potencialmente activas: Boletín de la Sociedad Geológica Mexicana, 1, 1-11.

Ramírez-Herrera, M.T., 1998, Geomorphic assessment of active tectonics in the Acambay Graben, Mexican volcanic belt: Earth Surface Processes and Landforms, 23(4), 317-332.

Reimer, P.J., Bard, E., Bayliss, A., Beck, J.W., Blackwell, P.G., Ramsey, C.B., Buck, C.E., Cheng, H., Edwards, R.L., Friedrich, M., Grootes, P.M., Guilderson, T.P., Haflidason, H., Hajdas, I., Hatte, C., Heaton, T.J., Hoffmann, D.L., Hogg, A.G., Hughen, K.A., Kaiser, K.F., Kromer, B., Manning, S.W., Niu, M., Reimer, R.W., Richards, D.A., Scott, E.M., Southon, J.R., Staff, R.A., Turney, C.S.M., Van der Plicht, J., 2013, Intcal13 and Marine13 Radiocarbon Age Calibration Curves 0–50,000 years Cal BP: Radiocarbon, 55(4), 1869-1887, https://doi.org/10.2458/azu_js_rc.55.16947.

Roldán-Quintana, J., Aguirre-Díaz, G.J., Rodríguez-Castañeda, J.L., 2011, Depósito de avalancha de escombros del volcán Temascalcingo en el graben de Acambay, Estado de México: Revista Mexicana de Ciencias Geológicas, 28(1), 118-131.

Sánchez-Garcilazo, V., 2000, Estudio de la Macrosismicidad del Estado de Michoacán: Morelia, Michoacán, México, Universidad Michoacana de San Nicolás de Hidalgo, tesis de maestría, 133 pp.

Scholz, C.H., 1990, The mechanics of earthquakes and faulting: New York, USA, Cambridge University Press, 439 pp.

Siebe, C., Guilbaud, M.N., Salinas, S., Kshirsagar, P., Chevrel, M.O., De la Fuente, J.R., Hernández-Jiménez, A., Godínez, L., 2014, Monogenetic volcanism of the Michoacán-Guanajuato Volcanic Field: Maar craters of the Zacapu basin and domes, shields, and scoria cones of the Tarascan highlands (Paracho-Paricutín region), *in* 5th International Maar Conference (5IMC-IAVCEI), Pre-meeting Field Guide (Nov. 13-17): Querétaro, México, Departamento de Vulcanología, Instituto de Geofísica, Universidad Nacional Autónoma de México, 33 pp.

Simon, J. J., Oosterhuis, L., Reneau Jr, R. B., 1987, Comparison of shrink-swell potential of seven ultisols and one alfisol using two defferent cole techniques1: Soil science, 143(1), 50-55.

Singh, S.K., Suárez, G., 1987, Overview of the seismicity of Mexico with emphasis on the September 1985 Michoacán earthquake, *in* Cassaro M.A., Martínez-Romero, E. (eds.), The Mexico Earthquakes-1985: Factors Involved and Lessons Learned: Washington, D.C., American Association of Civil Engineers, Proceedings of the International Conference of American Civil Engineering Society, 7-18.

Singh, S.K., Ordaz, M., Pérez-Rocha, L.E., 1996, The great Mexican earthquake of 19 June 1858: Expected ground motions and damage in Mexico City from a similar future event: Bulletin of the Seismological Society of America, 86(6), 1655-1666.

Singh, S. K., Iglesias, A., Ordaz, M., Pérez-Campos, X., Quintanar, L., 2011, Estimation of ground motion in Mexico City from a repeat of the M~ 7.0 Acambay earthquake of 1912: Bulletin of the Seismological Society of America, 101(5), 2015-2028.

Singh, S.K., Iglesias, A., Garduño, V.H., Quintanar, L., Ordaz, M., 2012, A source of the October, 2007 earthquake sequence of Morelia, Mexico and ground-motion estimation from larger earthquakes in the region: Geofísica Internacional, 51 (1), 73-86.

Stirling, M., Rhoades, D., Berryman, K., 2002, Comparison of Earthquake Scaling Relations Derived from Data of the Instrumental and Preinstrumental Era: Bulletin of the Seismological Society of America, 92(2), 812-830.

Suárez, G., García-Acosta, V., Gaulon, R., 1994, Active crustal deformation in the Jalisco block, Mexico: Evidence for a great historical earthquake in the 16th century: Tectonophysics, 234, 117-127.

Sunye-Puchol, I., Lacan, P., Ortuño, M., Villamor, P., Audin, L., Zúñiga, F.R., Langridge, R.M., Aguirre-Díaz, G.J., Lawton, T.F., 2015, La falla San Mateo: nuevas evidencias paleosismológicas de fallamiento activo en el graben de Acambay, México: Revista Mexicana de Ciencias Geológicas, 32(3), 361-376.

Suter, M., 2015, The AD 1567 M_w 7.2 Ameca, Jalisco, Earthquake (Western Trans-Mexican Volcanic Belt): Surface Rupture Parameters, Seismogeological Effects, and Macroseismic Intensities from Historical Sources: Bulletin of the Seismological Society of America, 105(2A), 646-656.

Suter, M., 2016, Structure and Holocene rupture of the Morelia fault, Trans-Mexican volcanic belt, and their significance for seismic-hazard assessment: Bulletin of the Seismological Society of America, 106(5), 2376-2388.

Suter, M., 2017, The 2 October 1847 MI 5.7 Chapala Graben Triggered Earthquake (Trans-Mexican Volcanic Belt, West-Central Mexico): Macroseismic Observations and Hazard Implications: Seismological Research Letters, 89(1), 35-46, DOI: 10.1785/0220170101.

Suter, M., Quintero-Legorreta, O., Johnson, C.A., 1992, Active faults and state of stress in the central part of the Trans-Mexican Volcanic Belt, Mexico; 1, The Venta de Bravo Fault: Journal of Geophysical Research, 97, 11983-11993.

Suter, M., Carrillo-Martínez, M., Quintero-Legorreta, O., 1996, Macroseismic study of earthquakes in the central and eastern parts of the Trans-Mexican Volcanic Belt: Bulletin of the Seismological Society of America, 86, 1952-1963.

Suter, M., López-Martínez, M., Quintero-Legorreta, O., Carrillo-Martínez, M., 2001, Quaternary intra-arc extension in the Central Trans-Mexican volcanic belt: Geological Society of America Bulletin, 113(6), 693-703.

Urbina, F., Camacho, H., 1913, La zona megasísmica Acambay-Tixmadejé, Estado de México, conmovida el 19 de noviembre de 1912: Boletín de Instituto Geológico de México, 32, 125 pp.

Velázquez-Bucio, M.M., Garduño-Monroy, V.H., 2018, Soft-sediment deformation structures induced by seismic activity in the San Pedro el Alto area, Acambay graben, Mexico: Revista Mexicana de Ciencias Geológicas, 35(1), 28-40.

Wells, D.L., Coppersmith, K.J., 1994, New empirical relationships among magnitude, rupture length, rupture width, rupture area, and surface displacement: Bulletin of the Seismological Society of America, 84, 974-1002.

Wesnousky, S.G., 2008, Displacement and geometrical characteristics of earthquake surface ruptures: Issues and implications for seismic-hazard analysis and the process of earthquake rupture: Bulletin of the Seismological Society of America, 98(4), 1609-1632.

Zúñiga, F.R., Pacheco, J.F., Guzmán-Speziale, M., Aguirre-Díaz, G.J., Espíndola, V.H., Nava, E., 2003, The Sanfandila earthquake sequence of 1998, Querétaro, Mexico: activation of an undocumented fault in the northern edge of central Trans-Mexican Volcanic Belt: Tectonophysics, 361(3), 229-238.

Manuscript received: november 29, 2018
Corrected manuscript received: april 5, 2019
Manuscript accepted: april 12, 2019